Iraqi Journal of Physics, 2022
DOI: 10.30723/ijp.v20i2.983

Vol.20, No.2, PP.53-63
P-ISSN: 2070-4003
E-ISSN: 2664-5548

Synthesis and Characterization of Ternary $Be_xZn_{1-x}O$ Nano Thin Films prepared by Pulsed Laser Deposition Technique

Ali L. Abed[a]*, Mohammed T. Hussein[b]
Department of Physics, College of Science, University of Baghdad, Baghdad, Iraq
[b]E-mail: mohammedtake@gmail.com
[a]*Corresponding author: ali.hasan1104@sc.uobaghdad.edu.iq

Abstract

Beryllium Zinc Oxide ($Be_xZn_{1-x}O$) ternary nano thin films were deposited using the pulsed laser deposition (PLD) technique under a vacuum condition of 10^{-3} torr at room temperature on glass substrates with different films thicknesses, (300, 600 and 900 nm). UV-Vis spectra study found the optical band gap for $Be_{0.2}Zn_{0.8}O$ to be (3.42, 3.51 and 3.65 eV) for the (300, 600 and 900nm) film thicknesses, respectively which is larger than the value of zinc oxide ZnO (3.36eV) and smaller than that of beryllium oxide BeO (10.6eV). While the X-ray diffraction (XRD) pattern analysis of ZnO, BeO and $Be_{0.2}Zn_{0.8}O$ powder and nano-thin films indicated a hexagonal polycrystalline wurtzite structure. The crystal structure showed a preferential orientation line at (101). Besides the nano thin film $Be_{0.5}Zn_{0.5}O$ has all orientations of ZnO and BeO. Moreover, the calculated average crystallite size for nano thin film was 16.48 nm. The surface morphology of the nano thin films investigated by atomic force microscope (AFM) showed a decrease in the average grain sizes (94.8, 79.2 and 59.4 nm) with the increase of films thickness due to quantum confinement effect.

Article Info.

Keywords:
ternary semiconductor, $Be_xZn_{1-x}O$, nano thin films,opticalproperties, PLD.

Article history:
Received: Feb. 27, 2022
Accepted: Apr. 7, 2022
Published: Jun. 01,2022

1. Introduction

Zinc oxide (ZnO) is one of the most important II-VI semiconductor compounds and has unique properties [1]. Furthermore, because of its exceptional electrical and optical properties, its direct bandgap of 3.37 eV and its excitons binding energy of about 60 meV at R.T, ZnO has been reported as a good candidate for ultraviolet range optoelectronic device applications [2, 3]. In the last decade, the band gap of ZnO has been modulated by alloying with other II-VI oxide semiconductors such as MgO, BeO, etc., and this has been studied by many researchers [4]. In recent times, beryllium oxide (BeO), with a wide direct bandgap of 10.6 eV, has been suggested as a good candidate to prevent the difficulties in the ZnO/MgO system, as the crystal structure is hexagonal for both ZnO and BeO. The well-known phase segregation was not found between ZnO and BeO with different values of Be concentration, so the energy bandgap could be controlled continuously from 3.3 to 10.6 eV by alloying BeO and ZnO with various percentage ratios [5, 6]. Consequently, BeO is considered

a suitable choice for energy band gap modulation in the manufacturing of optoelectronic devices based on ZnO. Depending on that, the structure and optical properties of the $Be_xZn_{1-x}O$ alloy have been the focus of many researchers [7-13]. Many techniques, such as radiofrequency magnetron sputtering, molecular beam epitaxy (MBE), chemical vapor deposition (CVD), and pulsed laser deposition (PLD), were used to deposit $Be_xZn_{1-x}O$ films, due to the high energy of the ablated particles in the plasma plume produced via laser interaction with target material [14, 15].

The aim of this work is to investigate adding a suitable concentration of BeO to ZnO then studies the optical, structural, and morphological properties of the $Be_xZn_{1-x}O$ nano thin films with different thickness and concentrations to obtain a wide energy band gap which satisfy the requirement applications.

2. Experimental work

$Be_xZn_{1-x}O$ thin films were deposited in a PLD system on glass substrates. The target of the compound $Be_xZn_{1-x}O$ was prepared, by mixing pure beryllium oxide and zinc oxide powder (of 99% purity), for three values of x (0.2, 0.5 and 0.8). By cold pressing (of 6 ton), the target was transformed into pellets of 10 mm diameter, 2 mm thickness, and 1gram weight. The glass substrates were ultrasonically cleaned with ethanol, then placed parallel to the target surface on a holder at a distance 3 cm from the target ($Be_xZn_{1-x}O$ pellet) and at an angle of about 45 degrees made by the normal laser beam and the target. The substrate holder was in the optimum (adjustable) position for the plasma plume's center. A double frequency Q-switched Nd: YAG laser (532 nm) was used and operated at an energy of 500 mJ/pulse and a 6 Hz repetition rate under vacuum conditions (10^{-3} torr) using a rotary pump at room temperature. The BeZnO thin films were deposited at different thicknesses of (300, 600, and 900 nm). Film thickness was measured using the interferometer fringes method, which is an application of Fizeau fringes equal spacing using a diode laser of 532.8 nm wavelength. With a UV-Vis spectrophotometer (Shimadzu 1800), the optical properties of $Be_xZn_{1-x}O$ thin films at room temperature were characterized. X-ray diffraction (XRD) pattern conducted with an X-ray diffractometer (XRD-6000 Labx, made by Shimadzu) with a radiation source (Cu Kα X-ray) of λ=1.5406 Å. Finally, the surface profile morphology of $Be_{0.5}Zn_{0.5}O$ thin films was observed with an Atomic Force Microscope (AFM)(CSPM AA3000 AFM supplied by Angstrom Company).

3. Results and discussion

3.1. Optical properties

The absorbance spectra for different films thicknesses (300, 600, and 900 nm) are shown in Fig.1. It is clear that the optical absorption edge has appeared in the UV region and shifted to a shorter wavelength with an increase in the film thickness, at (362, 353, and 339nm) for film thicknesses of (300, 600, and 900 nm), respectively. Furthermore, it is clear that the increase in absorbance is proportional to the increase in films thickness [16]. Based on these absorbance spectra, the absorption coefficients, α, of the films were determined by applying the following equation [17]:

$$\alpha = 2.303 \frac{A}{t} \quad \textbf{(1)}$$

where A and t are the absorbance and the thin film thickness, respectively. Fig.2 presents the absorption coefficient against wavelength for $Be_{0.2}$ $Zn_{0.8}$ O thin films of 300, 600, and 900 nm thicknesses. The absorption coefficient curves were of a similar behavior to that of the absorbance (A) curves. They showed a sharp absorption edge at wavelengths (363, 353, and 339 nm) with maximum magnitudes of α (1.6×10^4, 1.4×10^4 and 0.9×10^4) cm^{-1} for the thicknesses (300, 600, and 900 nm), respectively. This indicates a high probability of allowed direct transition [18]. According to Beer-Lambert law increase concentration in gas phase or increase of the film thickness in solid state, means more light is absorbed and decrease transmittance i.e. the intensity of absorption is increased which causes a blue shift that depends on the nature of the matter. This agrees with Nithya and Radhakrishnan [16].
Linear fitting extrapolation was used to find the optical energy band gap E_g which was calculated using Tauc's equation [19]:

$$\alpha h\nu = B(h\nu - E_g)^n \qquad \textbf{(2)}$$

where hν is the energy of incident photon, B is a constant, E_g is the optical band gap energy, and n=½ is for the direct transition. The energy gap value of $Be_{0.2}$ $Zn_{0.8}O$ was 3.42 eV, 3.51eV and 3.65 eV for the film thicknesses (300, 600, and 900 nm), respectively (as listed in Table 1 and shown in Fig.3). These values shows that the ZnO energy gap of 3.36 eV has increased as a result of the BeO effect which is considered as a strong evidence for the existence of BeO in $Be_{0.2}$ $Zn_{0.8}$ O deposited thin films. The band gap energy of the $Be_xZn_{1-x}O$ can be tailored by alloying ZnO with BeO [20-22]. Moreover, as the thickness increases, the optical energy gap also increases which is in relation to the increase of the optical absorption [16, 18].

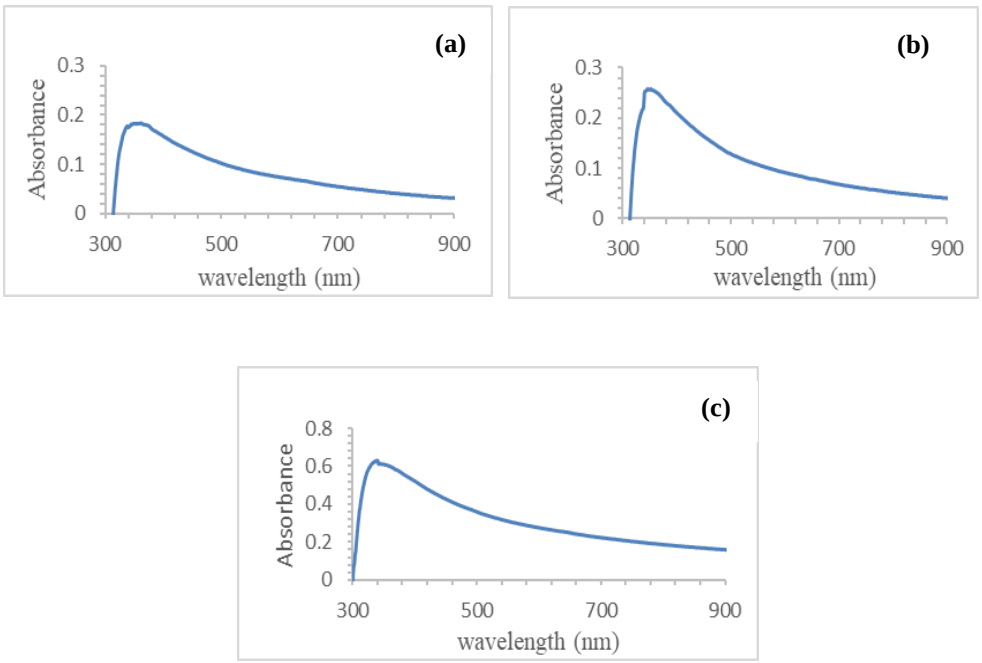

Figure 1: The absorbance spectra for $Be_{0.2}$ $Zn_{0.8}$ O with (a) 300 nm (b) 600 nm (c) 900 nm thicknesses.

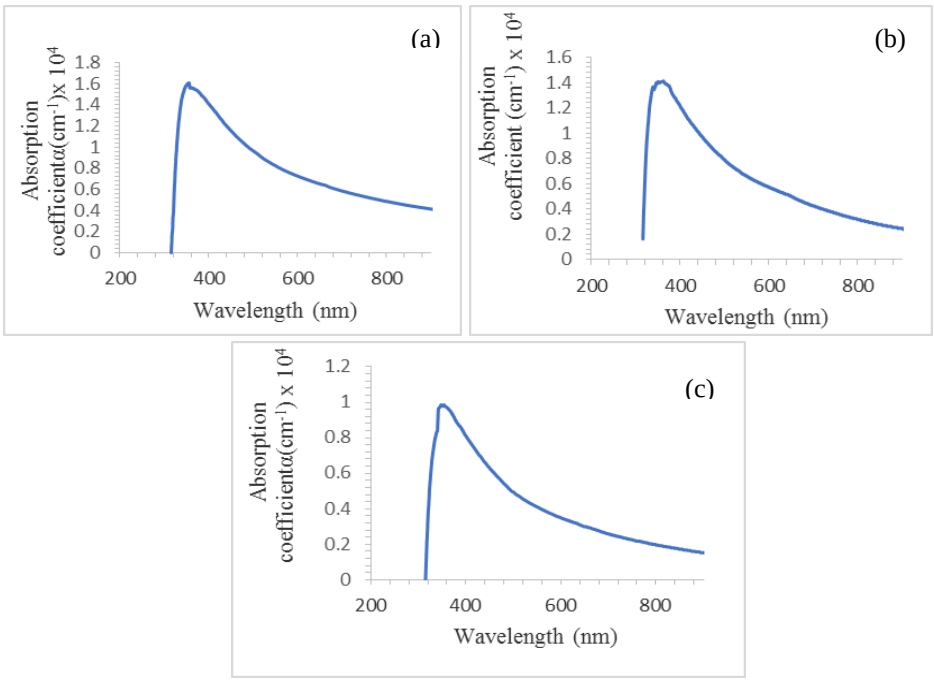

Figure 2: Absorption Coefficient against photon energy for $Be_{0.2}$ $Zn_{0.8}$ O thin Films with (a) 300, (b) 600, and (c) 900 nm thicknesses.

Table 1: The optical energy gaps for $Be_{0.2}$ $Zn_{0.8}$ O thin films of different thicknesses compared with bulk ZnO and BeO.

Film thickness (nm)	Optical Energy Gap E_g(eV)
300	3.42
600	3.51
900	3.65
ZnO Bulk[16]	3.3
BeO Bulk [11]	10.6

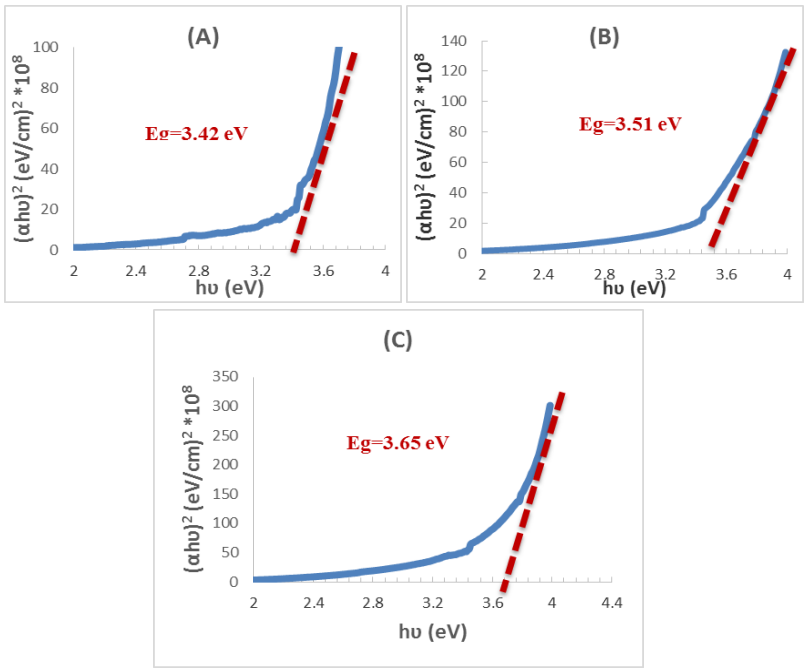

Figure 3: Plots of $(\alpha h\nu)^2$ as a function of photon energy ($h\nu$) for $Be_{0.2}Zn_{0.8}O$ thin film of (a) 300, (b) 600, and (c) 900 nm thicknesses.

3.2. Structural properties

The XRD analysis shown in Fig.4 was conducted for ZnO, BeO and $Be_{0.2}Zn_{0.8}O$ powder where the ICDD-Card no. for ZnO, and BeO is 36-1451, 43-1000, respectively. The indexed peaks positions were (100), (002), (101) belonging to ZnO at 2θ = 31.8°, 34.4°, and 36.2°, respectively and peaks of BeO for orientation (100),(002) and (101) were at 2θ = 38.6°, 41.3° and 43.9°, respectively, while $Be_{0.2}Zn_{0.8}O$ which combine all of the above orientations is illustrated with structural parameters in Table 2.

Table 2: Structural parameters for the ZnO, BeO and $Be_{0.2}Zn_{0.8}O$ powder.

hkl	*Peak position (2θ)*	*FWHM β (deg.)*	*Crystallite size D(nm)*	*Average crystallite size (nm)*
ZnO(100)	31.8	0.63	15.04	17.66
ZnO(002)	34.4	0.81	26.69	
ZnO(101)	36.2	0.538	15.58	
BeO(100)	38.6	0.49	17.92	18.46
BeO(002)	41.3	0.48	18.45	
BeO(101)	43.9	0.47	19.01	

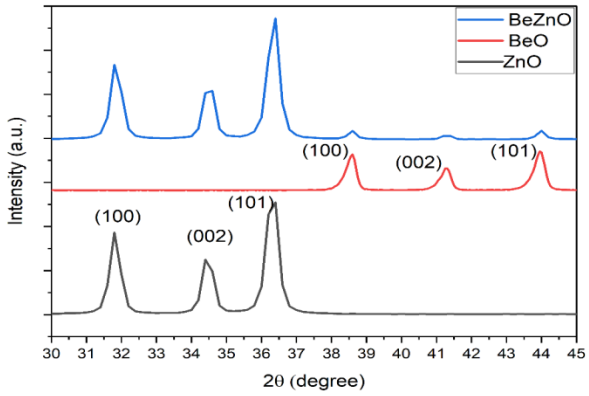

Figure 4: XRD peaks for the ZnO ,BeO and $Be_{0.2}Zn_{0.8}O$ powder.

Fig.5 shows XRD patterns for $Be_{0.2}Zn_{0.8}O$ nano thin films with different film thicknesses 300, 600 and 900 nm. They exhibit a strong peak at 2θ = 31.8°, 34.4°, and 36.2° for orientations (100), (002), and (101), respectively. It is clear that the crystallinity of the films improved with the increase of the film thickness.

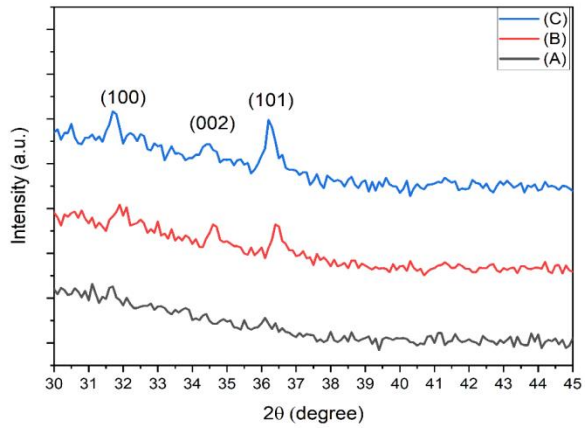

Figure 5: XRD peaks for the $Be_{0.2}Zn_{0.8}O$ thin films with different film thickness (A)300nm, (B)600nm and (C)900nm.

Fig.6 shows the crystallinity planes of BeZnO with different Be concentration ratio as ($Be_{0.2}Zn_{0.8}O$) , ($Be_{0.5}Zn_{0.5}O$) and ($Be_{0.8}Zn_{0.2}O$) to verify the influence of Be content on the crystalline structure for a selected film thickness of 900nm. Furthermore, as Be content was increased to 0.5, the diffracted peak intensity increased and showed strong peaks orientations but when Be content increased to 0.8 the BeO diffraction peak disappeared. This indicates a non-crystalline structure. Therefore, changes in the optical band gap energies to values greater than that of ZnO, indicates that Be atoms were well-substituted into Zn sites. Thus, the XRD results led us to consider that the Be atoms substituted the Zn in the crystal lattice [23, 24].

The crystallite sizes(D) of deposited films were measured by the Scherrer formula Eq.(3) [20]:

$$D = \frac{0.9\,\lambda}{\beta \cos\theta} \qquad \textbf{(3)}$$

where λ is the wavelength (1.5406Å) of X-ray, β is full width at half maximum (FWHM) (in radians units) and θ is the diffraction angle of the peak. The calculated results are listed in the Table 3.

The results show a decrease in crystallite size as the Be concentration in the composite films increases. Beryllium oxide has a smaller molecular size than Zinc oxide, where lattice constant of BeO (2.698 Å, hexagonal) and ZnO (3.249 Å, hexagonal) which results in a smaller crystallite [24].

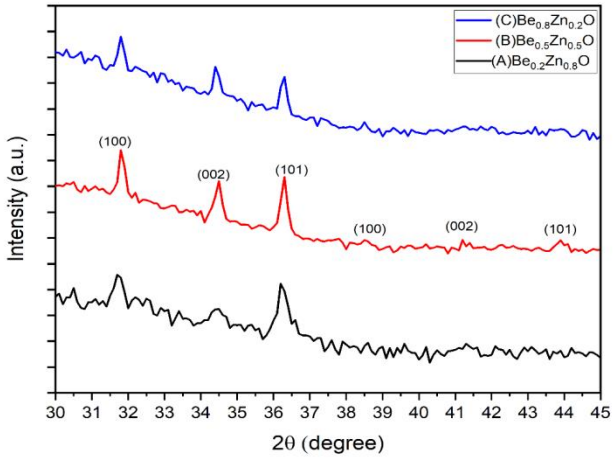

Figure 6: X-ray diffraction pattern for nano thin films thickness of 900nm with different Be concentrations (A)$Be_{0.2}Zn_{0.8}O$, (B)$Be_{0.5}Zn_{0.5}O$ and (C)$Be_{0.8}Zn_{0.2}O$.

Table 3: Structural parameters for the, $Be_{0.5}Zn_{0.5}O$ thin film for 900nm film thickness.

hkl	*Peak position (2θ)*	*FWHM β (deg.)*	*Crystallite size D(nm)*	*Average crystallite size (nm)*
(100)	31.7	0.63	13.7	16.48
(002)	34.4	0.52	16.7	
(101)	36.3	0.52	16.8	
(100)	38.5	0.4	21.9	
(002)	41.3	0.6	14.7	
(101)	43.9	0.6	14.89	

3.3. Morphological properties

The non-contact mode atomic force microscope (AFM) was employed to characterize the surface profile morphology of the $Be_{0.2}Zn_{0.8}O$ thin films. As shown in Fig.7, the morphology of the surface of the grown $Be_{0.2}Zn_{0.8}O$ thin films show low roughness as the film thickness increases [25, 26]. The uniformity of grain sizes on the surfaces of the films was consistent with the XRD results.

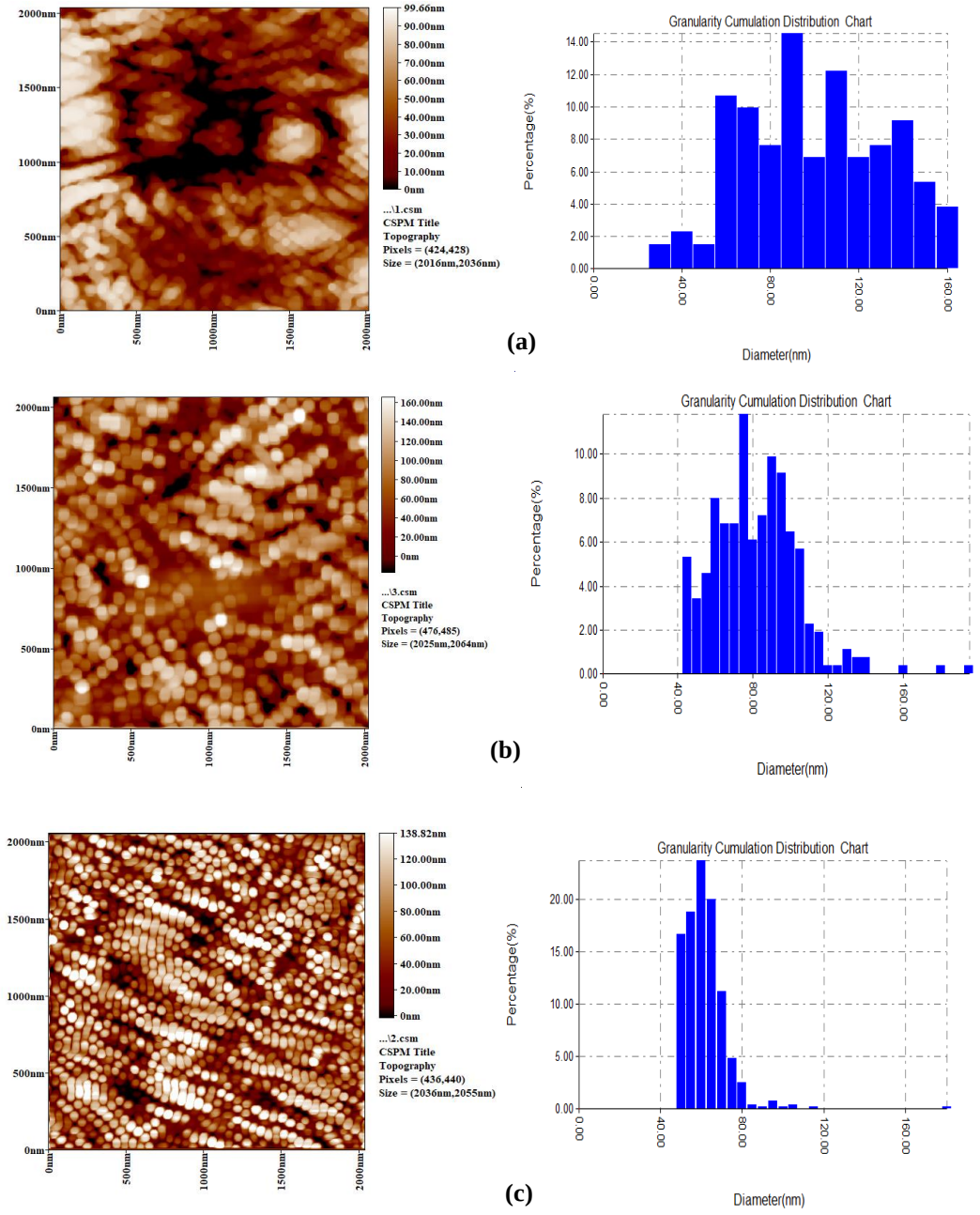

Figure 7: 2D AFM images of deposited $Be_{0.2}Zn_{0.8}O$ thin films with different thicknesses (a) 300nm, (b) 600nm, and (c) 900nm with granularity cumulative distribution chart.

Fig.8 shows AFM 3D images of deposited $Be_{0.2}Zn_{0.8}O$ thin films scanned over $1.5\times1.5\mu m^2$. There are two significant differences between them, namely grain size and surface roughness. The surface for 300 nm film thickness consisted of several big

grain sizes, so the average diameter was 94.8 nm and the root mean square (RMS) roughness was 27.3 nm. The surface of the 600 nm film thickness showed many small grain sizes 79.2nm and (RMS) 40nm. Lastly, with a film thickness of 900nm, an increase of the average diameter to 59.5 nm and the RMS roughness was 41 nm were noticed, as listed in Table 4.

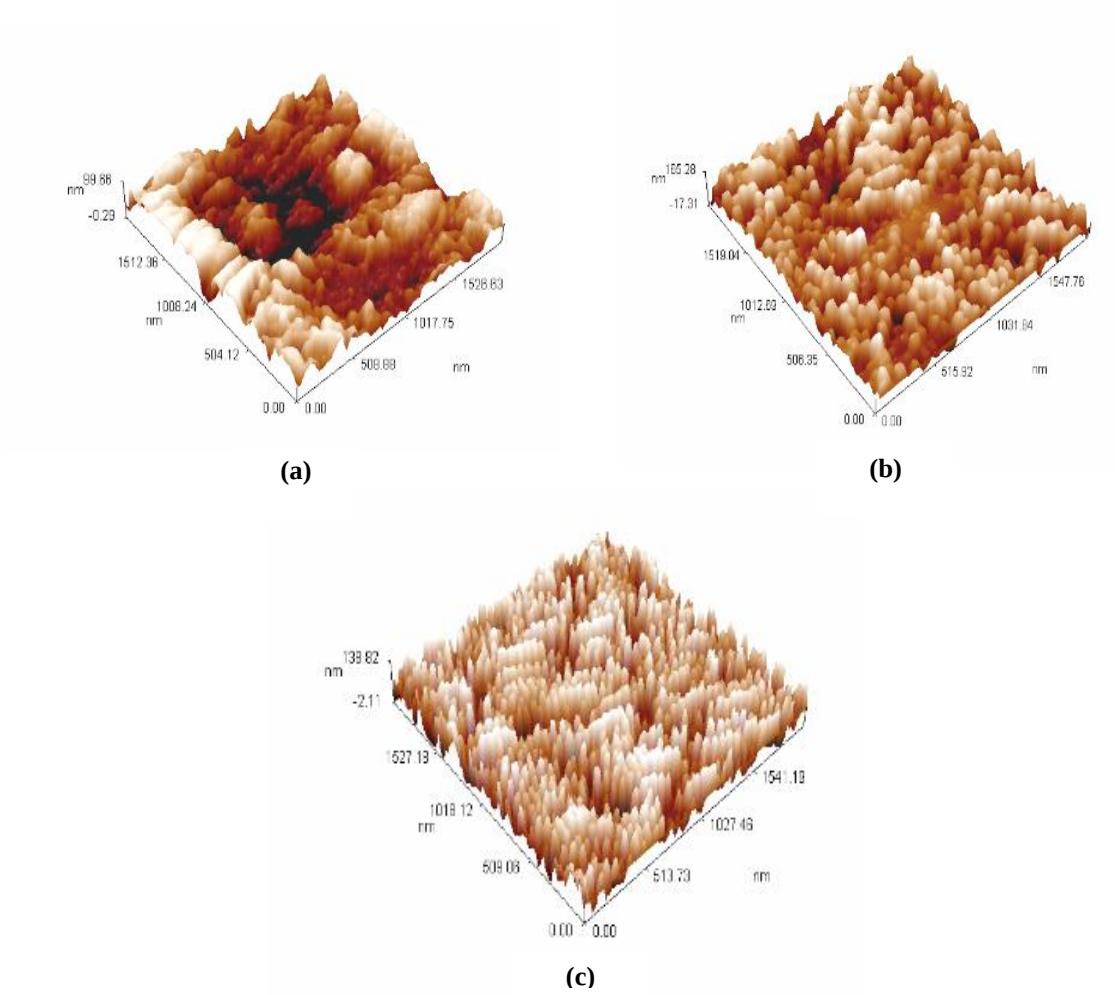

Figure 8: 3D AFM images of deposited $Be_{0.2}Zn_{0.8}O$ thin films with different thicknesses (a) 300nm, (b) 600nm, and (c) 900nm.

Table 4: AFM morphology parameters for BeZnO films.

Film thickness (nm)	*Average particle size (nm)*	*Average roughness (nm)*	*RMS (nm)*
300	94.8	23	27
600	79.2	32	40
900	59.4	35	41

4. Conclusions

Ternary nano thin films $Be_xZn_{1-x}O$ were prepared via pulsed laser deposition on a glass substrate with different thicknesses and concentrations. It was found that with the presence of Be, the energy gap has increased. Moreover, it was observed that with increasing the thickness, the grain size has decreased and the energy gap increased,

this is due to the quantum confinement effect. Finally, both BeO and ZnO have hexagonal crystal structures this leads to a decrease in the phase segregation between BeO and ZnO to form $Be_xZn_{1-x}O$ with a wide energy band gap which satisfy the requirement applications.

Acknowledgements

The author's would like to thank the Nanotechnology and Advanced Material Research Center, University of Technology, Baghdad-Iraq and Department of Physics, College of Science, University of Baghdad for their help and support in carrying out this research.

Conflict of interest

Authors declare that they have no conflict of interest.

References

1. Jalil Z. *Structural and optical properties of zinc oxide (ZnO) based thin films deposited by sol-gel spin coating method*. in *Journal of Physics: Conference Series*. 2018. IOP Publishing.
2. Qin L.-X., Liang H.-P., and Jiang R.-L., *Structural Transition from Ordered to Disordered of BeZnO2 Alloy.* Chinese Physics Letters, 2020. **37**(5): pp. 1-4.
3. Xiong D., He M., Wang Q., and Feng Z. *A DFT+ U Study On The Structural And Electronic Properties Of BeZnO alloys*. in *2nd International Forum on Management, Education and Information Technology Application (IFMEITA 2017)*. 2018. Atlantis Press.
4. Su L., Zhu Y., An Y., Xie J., and Tang Z., *Alloying induced disorder and localized excitonic states in ternary BexZn1− xO thin films.* Journal of Alloys Compounds, 2021. **874**: pp. 1-35.
5. Toporkov M., Ullah M., Demchenko D., Avrutin V., Morkoç H., and Özgür Ü., *Effect of oxygen-to-metal flux ratio on incorporation of metal species into quaternary BeMgZnO grown by plasma-assisted molecular beam epitaxy.* Journal of Crystal Growth, 2017. **467**: pp. 145-149.
6. Bouziani I., Kibbou M., Haman Z., Benhouria Y., Essaoudi I., Ainane A., and Ahuja R., *Electronic and optical properties of ZnO nanosheet doped and codoped with Be and/or Mg for ultraviolet optoelectronic technologies: density functional calculations.* Physica Scripta, 2019. **95**(1): pp. 1-14.
7. Wentao E., Li M., Meng D., Cheng Y., Fu W., Ye P., and He Y., *High-performance amorphous BeZnO-alloy-based solar-blind ultraviolet photodetectors on rigid and flexible substrates.* Journal of Alloys Compounds, 2020. **831**: pp. 1-7.
8. Su L., Chen H., Xu X., and Fang X., *Novel bezno based self-powered dual-color uv photodetector realized via a one-step fabrication method.* Laser Photonics Reviews, 2017. **11**(6): pp. 1-9.
9. Yıldırım H., *Dispersion relations of interface and quasi-confined phonon modes in ZnO/BeZnO quantum wells.* Physics Letters A, 2021. **385**: pp. 1-7.
10. Yu J., Kim J., Park D., Kim T., Jeong T., Youn C., and Hong K., *A study on structural formation and optical property of wide band-gap Be0. 2Zn0. 8O layers grown by RF magnetron co-sputtering system.* Journal of crystal growth, 2010. **312**(10): pp. 1683-1686.

11. Chung J.-K., Kim W.-J., Kim S.S., Song T.K., and Kim C.J., *Structural and optical properties of Be-doped ZnO nanocrystalline films by pulsed laser deposition.* Thin Solid Films, 2008. **516**(12): pp. 4190-4193.
12. Kim J., Park D., Yu J., Kim T., Jeong T., and Youn C., *Emission mechanism of localized deep levels in BeZnO layers grown by hybrid beam method.* Journal of materials science, 2008. **43**(9): pp. 3144-3148.
13. Mustafa S.K., Jamal R.K., and Aadim K.A., *Studying the effect of annealing on optical and structure properties of ZnO nanostructure prepared by laser induced plasma.* Iraqi Journal of Science, 2019: pp. 2168-2176.
14. Wang Y.-C., Su L.-X., Zhao Y., Liu J.-F., Shen Z.-C., Feng Y.-H., Wu T.-Z., and Tang Z.-K., *Resonant Raman scattering study of Be x Zn 1− x O thin films grown on sapphire by molecular beam epitaxy.* International Journal of Modern Physics B, 2017. **31**(16-19): pp. 1-6.
15. Sun X. and Kwok H.S., *Optical properties of epitaxially grown zinc oxide films on sapphire by pulsed laser deposition.* Journal of applied physics, 1999. **86**(1): pp. 408-411.
16. Nithya N. and Radhakrishnan S.R., *Effect of thickness on the properties ZnO thin films.* Advances in Applied Science Research, 2012. **3**(6): pp. 4041-4047.
17. Kumar K.B. and Raji P., *Synthesis and characterization of nano zinc oxide by sol gel spin coating.* Recent research in science technology, 2011. **3**(3): pp. 48-52.
18. Su L., Zhu Y., Zhang Q., Chen M., Wu T., Gui X., Pan B., Xiang R., and Tang Z.J.A.s.s., *Structure and optical properties of ternary alloy BeZnO and quaternary alloy BeMgZnO films growth by molecular beam epitaxy.* Applied surface science, 2013. **274**: pp. 341-344.
19. Salim M.A., *Effect of thickness on the optical properties of ZnO thin films prepared by pulsed laser deposition technique (PLD).* Iraqi Journal of Physics, 2017. **15**(32): pp. 114-121.
20. Han M., Kim J., Jeong T., Park J., Youn C., Leem J., and Ryu Y., *Growth and optical properties of epitaxial BexZn1− xO alloy films.* Journal of crystal growth, 2007. **303**(2): pp. 506-509.
21. Ryu Y., Lee T., Lubguban J., Corman A., White H., Leem J., Han M., Park Y., Youn C., and Kim W., *Wide-band gap oxide alloy: BeZnO.* Applied physics letters, 2006. **88**(5): pp. 1-2.
22. Zhang Y., Hao X., Huang Y., Tian F., Li D., Wang Y., Song H., and Duan D., *Structural and Electrical Properties of Be x Zn1–x O Alloys under High Pressure.* Chinese Physics Letters, 2021. **38**(2): pp. 1-5.
23. Ye D., Mei Z., Liang H., Liu Y., Azarov A., Kuznetsov A., and Du X., *Beryllium sites in MBE-grown BeZnO alloy films.* Journal of Physics D: Applied Physics, 2014. **47**(17): pp. 1-6.
24. Khoshman J., Jakkala P., Ingram D., and Kordesch M., *Optical conductivity tuning and electrical properties of a-BexZnyO thin films.* Journal of Non-Crystalline Solids, 2016. **440**: pp. 31-37.
25. Lin Y.-C., Wang B., Yen W., Ha C., and Peng C., *Effect of process conditions on the optoelectronic characteristics of ZnO: Mo thin films prepared by pulsed direct current magnetron sputtering.* Thin Solid Films, 2010. **518**(17): pp. 4928-4934.
26. Christoulakis S., Suchea M., Koudoumas E., Katharakis M., Katsarakis N., and Kiriakidis G., *Thickness influence on surface morphology and ozone*

sensing properties of nanostructured ZnO transparent thin films grown by PLD. Applied surface science, 2006. **252**(15): pp. 5351-5354.

تحضير وتشخيص الأغشية الثلاثية $Be_xZn_{1-x}O$ النانوية المحضرة بتقنية الترسيب بالليزر النبضي

على لائق عبد، محمد تقي حسين
قسم الفيزياء، كلية العلوم، جامعة بغداد، بغداد، العراق

الخلاصة

تم تحضير أغشية نانوية ثلاثية لأوكسيد البريليوم زنك ($Be_xZn_{1-x}O$) بتقنية الترسيب بالليزر النبضي تحت ضغط منخفض يصل الى 10^{-3} تور في درجة حرارة الغرفة على قواعد زجاجية وباسماك مختلفة (300 و 600 و 900 نانومتر).من خلال دراسة أطياف الاشعة الفوق بنفسجة والمرئية والتي اعطت قيمة فجوة الطاقة (3.42 و 3.51 و 3.65 الكترون-فولت) والتي هي اكبر قيمة من قيمة فجوة الطاقة لاوكسيد الزنكZnO (3.36الكترون-فولت) وبنفس الوقت اصغرمن قيمة فجوة الطاقة لاوكسيد الريليوم BeO (10.6الكترون - فولت). بينما اوضحت نتائج حيود الاشعة السينية الخصائص التركيبية لكل من أوكسيد الزنك ZnO واوكسيد البريليوم BeO وكذلك الاوكسيد البريليوم- زنك $Be_{0.2}Zn_{0.8}O$ للطور الافضل (101) كمسحوق ذو تركيب سداسي ورتزايت متعدد التبلور.بينما لغشاء أوكسيد البريليوم –زنك $Be_{0.5}Zn_{0.5}O$ يحتوي على كل متجهات ZnO و BeO وبمعدل حجم بلوري (16.48نانومتر). تمت دراسة الخصائص المورفولوجية للسطح للأفلام النانوية بواسطة مجهر القوى الذرية (AFM) والذي اظهر نقصان في قيمة معدل الحجم الحبيبي (94.8 و 79.2 و 59.4 نانومتر) مع زيادة السمك وذلك نتيجة تأثير الحصر الكمي.